

1. Large Helical Device (LHD) Project

Research on confining high-temperature plasmas with magnetic fields is being conducted around the world with the aim of realizing nuclear fusion power generation. At the Large Helical Device (LHD) of the National Institute for Fusion Science, a "deuterium plasma experiment" has been conducted since 2017 to generate plasma, using deuterium. In FY2020, we succeeded in generating plasma with both electron and ion temperatures reaching 100 million degrees. With this success, the LHD research has entered a new stage. In FY2021, we conducted experiments on mixed hydrogen isotope plasmas of "deuterium" and "hydrogen" to simulate the mixed hydrogen isotope plasmas of "deuterium" and "tritium" that will be used in future fusion power generation. This experiment has produced results that will form the basis of future fusion research, such as the world's first observation of mixed hydrogen isotopes. We also focused on the physics of multi-ions, including helium, which will be the ash of future nuclear fusion reactions in fusion power plants.

The realization of fusion power generation requires the stable maintenance of such a high-temperature plasma for a long period of time, and there are many issues to be solved to maintain this stability. Plasma confined by a magnetic field must be kept at a high temperature of more than 100 million degrees Celsius in the center where the fusion reaction takes place, while the plasma in the periphery must be kept as cool as possible, to reduce the heat load on the walls of the device that confines the plasma. This temperature gradient is extremely steep, 100 million degrees in about one meter. This causes turbulence, with various sizes of vortices stirring the plasma, resulting in a low center temperature. In addition, when the plasma pressure gradient becomes steep, the plasma becomes unstable, and a part of it which is may be lost (this phenomenon is called instability). Therefore, it is necessary to understand turbulence and instability and to establish methods to control them in order to maintain plasma stability.

Physics experiments on plasma turbulence and instability have provided important insights into the development of control methods for turbulence and instability in future fusion plasmas. Turbulence and sudden instabilities are considered to be deeply related not only to fusion plasmas but also to various phenomena occurring in space and on the earth. We are planning to promote such interdisciplinary research in LHD. Spectroscopy is a powerful tool to investigate the turbulence and instability in high-temperature plasma since it is also widely used in the other scientific field of space and solar plasma physics in. Therefore, the development of the spectroscopy technique should have a strong academic impact on improving the observation technique.

We have four topical groups to proceed with the interdisciplinary research in LHD.

1) multi-ion plasma, 2) turbulence, 3) spectroscopy, 4) instability. In FY2021, we had 115 principle proponents of the LHD experiment, including NIFS staff, domestic collaborators, and overseas (international) collaborators. Proponents outside NIFS exceeded 50% of the total, as seen in Fig.1.

Significant progress in scientific research has been made in experiments on turbulence/transport, magnetic islands, energetic particles, spectroscopy, and machine learning based on international and domestic collaborations. LHD experiments show the importance of

- 1) Role of turbulence spreading
- 2) Core-edge-divertor coupling (non-local transport)
- 3) Non-diffusive transport (especially heat transport)
- 4) Interaction between magnetic islands (MHD) and transport

Please visit https://www-lhd.nifs.ac.jp/pub/Science_en.html

Based on the LHD experiment in 2021, we released the results when scientific papers were published in high-impact journals such as Nature Physics or Physical Review Letters.

Please visit the NIFS home page at https://www.nifs.ac.jp/en/news/index_list.html.

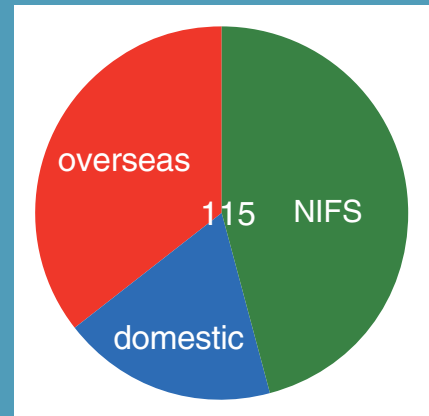


Fig. 1 Fraction of the number of overseas, domestic, and NIFS researchers proponents.

(K. Ida)

Multi-ion

Highlight

Progress in the research in multi-ion plasmas

A deuterium (D) - tritium (T) fusion reaction will produce helium (He, $Z = 2$) as a by-product. Therefore, in a possible D-T fusion reactor, we must control the plasma efficiently and effectively, consisting as it does of multi-ions, such as hydrogen isotopes and impurities (impurities other than He would come from the plasma-facing components). One of the critical issues in D-T fusion plasma is to control the radial profile of each hydrogen isotope and impurities in that mixed plasma, so that it achieves sustained nuclear fusion burning. High confinements of hydrogen isotopes and high pumping efficiency of He must be performed simultaneously. To gain the insight needed to achieve such a conflicting capability, we have strategically promoted the research on multi-ion plasmas from the FY2021 experiment campaign of the Large Helical Device (LHD). In the study on multi-ions, we identified the confinement study of thermalized and high-energy He by using an He-beam as a high priority. For such studies, one of the perpendicular NBIs (NBI#5) was modified to allow the injection of the He beam. We successfully measured the spatiotemporal behaviors of fast and thermalized He ions, introduced by the He-beam in the LHD plasma, with charge exchange spectroscopy (CX, FICXS) diagnostics. Figure 1 shows an example of a waveform summary of the LHD plasma with He-beam injection. Due to the He-beam injection, we observed an increment of charge exchange He II line intensity. And we also observed the increments of line-averaged electron density and central ion temperature due to the He-beam injection. However, we found that the following points make the study of beam-derived He transport difficult and problematic: the He gas inflow from the NBI#5 device and the He recycled from the plasma-facing components (divertor). We are working on solving these problems by devising new experimental methods and further modifications and improvements to the experimental apparatus.

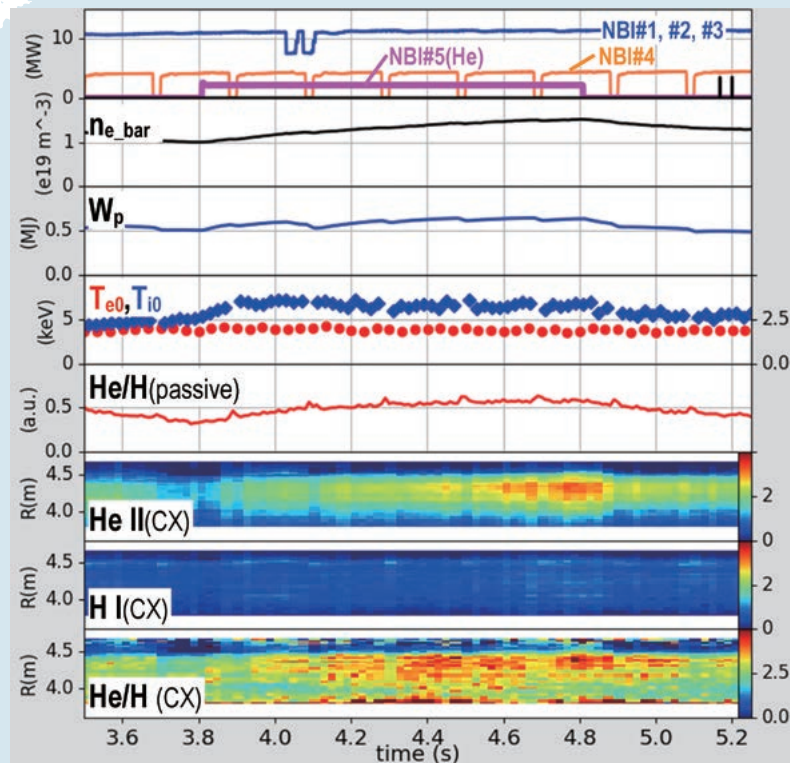


Fig. 1 Example of waveform summary of the LHD plasma with He-beam injection. Here the He-beam was injected from $t = 3.8$ s until $t = 4.8$ s. As can be seen in the third frame from the bottom, charge exchange He II line intensity was increased during the He-beam injection, mainly around $R = 4.3$ m. Also, the line-averaged electron density (the second frame from the top) and central ion temperature (the fourth frame from the top) were increased due the He-beam injection.

(N. Tamura)

Good core plasma performance realized in deuterium plasmas compatible with heat load mitigation at the plasma facing components

In fusion reactors it is necessary to generate and maintain as high a temperature as possible in the core confinement plasma to accelerate a fusion reaction, while heat flux from the confined plasma can damage or melt the plasma facing wall. The solution to this problem is to make the plasma at the edge as cold as possible, to reduce the heat load on the wall. In many cases, however, the energy of the confined plasma is also reduced simultaneously.

In the Large Helical Device (LHD), we have been working with the aim of solving this problem. One way to do this was to create a magnetic field structure called a “magnetic island” in the peripheral region, as shown in Fig. 2 (a), and to separate the cold edge plasma from the hot plasma in the confinement region [1, 2, 3]. It has been shown that when the magnetic island is formed, plasma energy is converted to radiation in the magnetic island and the plasma in the island becomes colder. Consequently the heat load on the device wall is dispersed in a wide area, reducing the peak heat load.

On the other hand, since future fusion reactors will use deuterium and tritium plasmas to generate electricity, it is necessary to investigate how the plasma changes, depending on the hydrogen isotopes. In this experiment, we have compared the operation of deuterium and hydrogen plasmas using the magnetic island described above. As a result, it was observed in the deuterium plasmas, that the energy density (pressure = temperature \times density) of the confined plasma increased even when the plasma temperature in the peripheral region decreased, as shown in Fig. 2 (a). When this phenomenon occurs, the plasma fluctuation is reduced, and the temperature and density profiles of the plasma at the boundary between the magnetic island and the confined plasma become steeper, leading to a good confinement of plasma. This phenomenon is more pronounced in the deuterium plasmas than in the hydrogen plasmas, as shown in Fig. 2 (b), where the deuterium plasmas show higher radiated power, compatible with good core plasma confinement [4]. The results indicate that deuterium plasmas can achieve higher performance of confined plasmas than hydrogen ones, while reducing the peak heat load on the plasma facing wall.

The results show that future deuterium and tritium plasmas may be able to reduce the heat load on the device wall, while maintaining higher plasma performance.

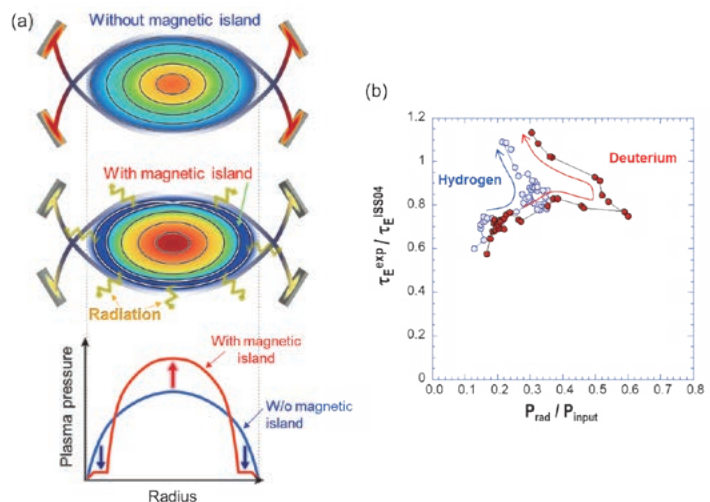


Fig. 2 (a) The plasma cross section in the Large Helical Device (LHD) without (top) and with (middle) a magnetic island. (bottom) The plasma pressure profile without and with a magnetic island. With one, the plasma energy is converted to radiation in the island and the plasma becomes colder there (middle figure). As a result, the heat load on the device wall is dispersed and the peak heat load decreases. At the same time a steep temperature and density gradient is created in the edge region, which increases plasma energy in the confined region (bottom figure). (b) Energy confinement scaling factor as a function of the radiated power with the edge magnetic island. The red and blue symbols show the deuterium and the hydrogen plasmas, respectively. The arrows in the figure indicate time sequence of the discharges.

(M. Kobayashi)

- [1] S.N. Pandya *et al.*, Nucl. Fusion **56**, 046002 (2016).
- [2] M. Kobayashi *et al.*, Nucl. Fusion **59**, 096009 (2019).
- [3] T. Oishi *et al.*, Plasma Fus. Res. **17**, 2402022 (2022).
- [4] M. Kobayashi *et al.*, Nucl. Fusion **62**, 056006 (2022).

Control of plasma particles by powerful vacuum pumping [5]

Fusion power generation is achieved by injecting hydrogen fuel into a high-temperature plasma of over 100 million degrees Celsius, where the injected hydrogen becomes high-temperature ions and undergoes a nuclear fusion reaction. The ionized hydrogen (fuel particles) is ejected out of the plasma, some bouncing off the plasma facing walls and back into the plasma, and some being ejected out of the vessel by a vacuum pump. The research team has experimented with the use of powerful cryogenic vacuum pumps in a system called a divertor, to reduce the amount of hydrogen returning to the plasma in experiments in the Large Helical Device (LHD).

In the divertor system, hydrogen fuel is drawn in to compress the hydrogen fuel. The experiment team systematically investigated the relationship between the cage of magnetic field lines that confine the plasma (magnetic field configuration) and the compression of neutral particles in the divertor. As a result, they found that the hydrogen fuel can be highly compressed in the divertor if the position of the center of the plasma (magnetic axis) is inward-shifted.

Next, plasma discharges were performed using a cryogenic vacuum pump inside the divertor in the magnetic configuration, with the inward-shifted magnetic axis. As a result, the density of the plasma was increasing without the cryogenic vacuum pump in the divertor, and eventually collapsed due to its uncontrollable density. On the other hand, the plasma density can be maintained at a constant level with the cryogenic vacuum pump in the divertor and successfully controlled. In addition, plasma heat transport analysis (another major achievement of this research was the creation of a heat transport analysis program) showed that energy confinement was better at the plasma core region when a cryogenic vacuum pump in the divertor was used. This established an easy and stable method for controlling hydrogen fuel. We expect that further progress will be made in our research toward maintaining steady-state fusion plasmas.

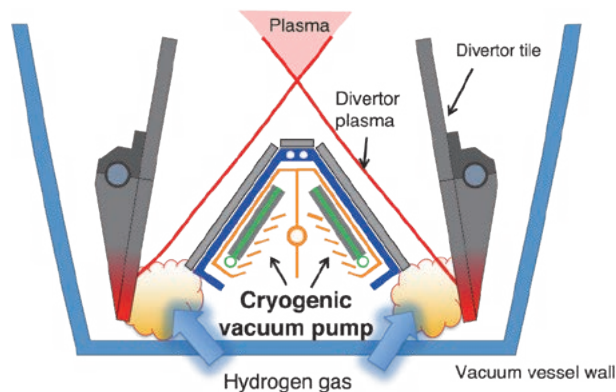


Fig. 3 At the periphery of the plasma confined by the magnetic field in the Large Helical Device (LHD), the plasma is drawn into a region called the divertor, where it becomes neutral gas. A cryogenic vacuum pump is installed inside the divertor to exhaust the neutral gas.

[5] G. Motojima *et al.*, Phys. Scr. **97**, 035601 (2022).

(G. Motojima)

Realization of stable heat load reduction on the wall, using two-species impurity gas injection [6, 7]

Stable and effective heat load reduction on the divertor was realized using neon (Ne) and krypton (Kr) injection, compared with single-species injection in the LHD. In fusion reactors, a fusion reaction occurs by confining high-temperature plasma exceeding 100 million Celsius degrees. Due to the flow of plasma from its high temperature core to a place called the “divertor” in the wall of the device, it is necessary to suppress the local heat load of the divertor. Therefore, an operational method called “divertor detachment” is being investigated, in which impurities are injected around the edge plasma and the heat load is dispersed as radiation. In the LHD, we conducted experiments on the divertor detachment.

In the divertor detachment experiments, one-species of impurity is usually injected. In the case of only seeding Ne, divertor detachment occurred; however, it could only be maintained for about 0.2 seconds, as shown in Fig. 4 (a) → (b) → (c). On the other hand, the LHD research group conducted the experiment using the injection of two species of impurities (Ne and Kr) to explore a more advanced operational method. As a result, we succeeded in stably maintaining the divertor detachment for about one second, as shown in Fig. 4 (a) → (d) → (e).

It was found that in the two-species injection, the radiation of Kr increased by Ne injection. Due to the phenomenon, the divertor heat load could be effectively reduced by the increase of plasma radiation with a smaller amount of impurities. Moreover, accumulation of the injected impurities toward the core plasma was suppressed. We also found that there are optimal conditions for the phenomenon regarding electron temperature and density around the edge plasma.

Since fusion reactors need to operate stably, it is necessary to maintain a stable divertor detachment. In addition, if the injected impurities for the divertor detachment are accumulated toward the core plasma, the fusion output power will decrease; therefore the influence of the impurities must be limited to the edge plasma. This result has provided important insights that will lead to the establishment of operational methods for divertor detachment.

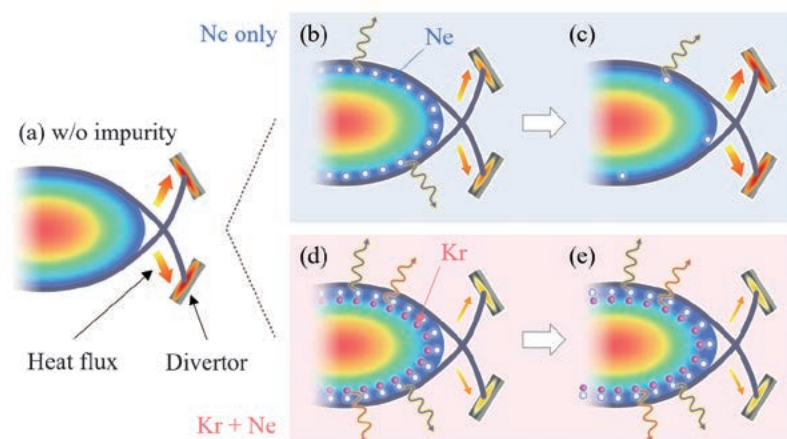


Fig. 4 (a) LHD plasma before impurity seeding. In the seeding of only Ne, (b) divertor heat load decreased with radiation enhancement just after the seeding; however, (c) divertor heat load increased again ~ 0.2 s after the seeding with a decrease of radiation. On the other hand, in the Kr+Ne seeding, (d, e) reduction of divertor heat load with radiation enhancement was maintained for ~ 1 s.

[6] K. Mukai *et al.*, Plasma Fusion Res. **15**, 1402051 (2020).

[7] K. Mukai *et al.*, Nucl. Fusion **61**, 126018 (2021).

TG2: Turbulence topical group

Highlight

Turbulence suppression by boron powder injection

We have discovered that sprinkling boron powder injection into the plasma reduces impurities from the walls and at the same time suppresses plasma turbulence. In order to realize fusion power generation, it is necessary to maintain stable high-temperature plasma. However, impurities generated from the walls of the vessel confining the plasma and turbulence generated in the plasma cause its temperature to drop. One way to prevent impurities entering the plasma is to form a boron film on the wall surface. In international cooperation with the Princeton Plasma Physics Laboratory (PPPL) in the United States, we have installed an impurity powder dropper (IPD) to inject boron and other powders onto plasma in LHD.

When boron powder is injected during plasma discharges from the IPD, it is found that a boron film is formed on the wall surface in real time, reducing impurities from the wall surface, suppressing heat loss from the plasma, and maintaining a stable high temperature state. In other plasma experimental devices, the temperature increase due to powder dispersal has been observed in a very short time, but LHD was able to maintain a stable state for a very long time. Why can such an advantageous plasma state be maintained? We measured plasma turbulence intensity and calculated computer simulation analysis. As a result, we found that the injection of boron powder suppresses the turbulence in the plasma. Figure 1(a) shows clear turbulence suppression in almost the whole radius. It might be caused by the effect of increasing flow shear. This achievement will greatly contribute to the establishment of a method for stably maintaining high-temperature plasma.

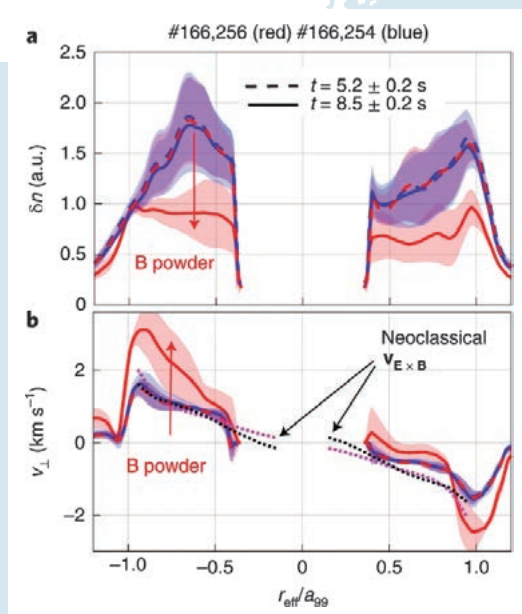


Fig. 1 Radial profiles of turbulent fluctuation amplitude δn (a) and the perpendicular velocity v_{\perp} (b) for a powder injection shot (#166,256, red) and its reference (#166,254, blue), at $t = 5.2$ s (before injection, dashed lines) and $t = 8.5$ s (during injection, solid lines). The radial profiles are averaged over a time window of 0.4 s, to avoid instantaneous variations caused by the pulsed diagnostic neutral beam. The shaded area accounts for the standard deviation in time. In b, neoclassical estimates of $\mathbf{E} \times \mathbf{B}$ velocity for #166,256 before (black) and during (magenta) powder injection are shown with dotted lines.

[1] F. Nespoli *et al.*, "Observation of a reduced-turbulence regime with boron powder injection in a stellarator", *Nature Physics* **18**, 350–356 (2022).

Plasma turbulence spreading by magnetic fluctuation reduces heat load on a fusion device wall

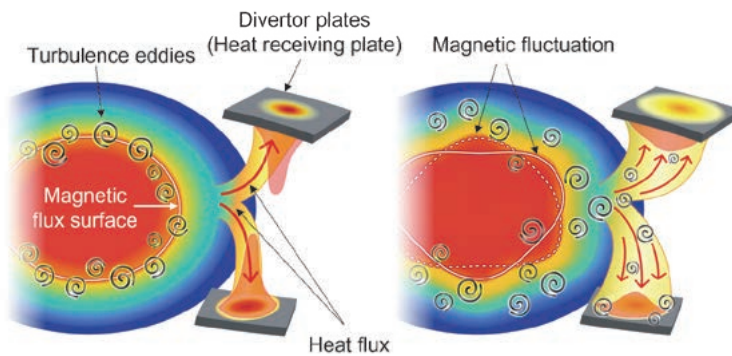


Fig. 1 Picture of turbulence spreading caused by magnetic fluctuation. Left: Turbulence generated in the plasma stays in the same place. A heat load is localized at the divertor plates and the peak value is high. Right: Magnetic field fluctuation occurs and turbulence propagates in the plasma. The heat flux to the divertor plate widens and the peak heat load decreases.

To achieve a nuclear fusion reactor, control of turbulence and the divertor heat load is mandatory. To understand and control the turbulence, it is necessary to clarify how turbulence is generated in the plasma, and how it propagates. However, the propagation of turbulence is not yet fully understood. In addition, to reduce the heat load on the divertor plates, impurity seeding has been studied to disperse the plasma energy to a wider area by radiation from the impurity ions. This method, however, has problems such as cooling of the confined plasma by impurity influx.

In LHD we have conducted experiments with RMP application, where a high temperature and steep density gradients develop at the edge region, simultaneously with their flat profile, adjacent to the gradient region. It has been observed that turbulence was generated in the region with the largest gradient and remained in the same place without propagating. At this time, the heat flowing out of the plasma was concentrated in a narrow area, and the divertor plate was subjected to an extremely large local load.

On the other hand, it has been found that when a magnetic fluctuation was excited around the steep gradient region, the turbulence propagated outward in the plasma. It was also found that the heat flux from the plasma to the divertor plates was scattered over a wide area by this turbulence. As a result, the peak divertor heat load decreased by a factor of about four, compared to a case without the magnetic field fluctuation. It was also confirmed that the center of the plasma remained at a high temperature and density state. Thus, with excitation of a magnetic fluctuation, it was discovered that the heat load could be reduced by propagating turbulence while maintaining a high central temperature and density in the plasma [1].

This result demonstrates a completely new method for controlling turbulence generated in plasmas and the heat load on the divertor plates.

[1] M. Kobayashi *et. al.*, “Turbulence spreading into an edge stochastic magnetic layer induced by magnetic fluctuation and its impact on divertor heat load”, *Phys. Rev. Lett.* **128**, 125001 (2022). DOI: 10.1103/PhysRevLett.128.125001

(M. Kobayashi, K. Tanaka, K. Ida, Y. Hayashi, Y. Takemura and T. Kinoshita)

Direct observation of the non-locality of non-diffusive counter-gradient electron thermal transport during the formation of hollow electron-temperature profiles in the Large Helical Device

Thermal transport is usually considered in a diffusion model where the heat flux is driven by a temperature gradient. In the Large Helical Device (LHD), an external heating method called electron cyclotron heating (ECH) is used, which can heat a narrow plasma region. Normally the plasma center is heated to produce a high-temperature plasma and a peaked electron temperature (T_e) profile. However, in this study [1] we observed for the first

time that heating away from the plasma center produces a hollow T_e profile; in a quasi-steady state where the T_e profile does not change, it is possible to describe the non-diffusive outward heat flux in terms of heat convection. Such a model can reproduce the T_e profile of the LHD plasma.

Next, we experimentally investigated the response of the T_e profile to a plasma with a hollow T_e profile when additional ECH was added to the center of the T_e profile, as shown in Fig. 1. In other words, the transient response of how the heat pulse propagates outward from the center was investigated from the time evolution of the T_e profile. The results showed that the heat pulse propagated transiently against the T_e gradient. Also, with core heating, the T_e profile changed from a hollow profile to a peaked one over time, but there was a period when it just flattened out (the T_e gradient became zero). Even then, net heat flowed outward; direct experimental investigation of the relationship between the T_e gradient and the driven heat flux showed that the diffusion model could not explain the heat transport in this case.

We then stopped the core heating and examined the relationship between the T_e gradient and driven heat flux when the T_e profile returned from the peak profile to the hollow one. Figure 2 shows that the trajectory was different from that during core heating. This phenomenon is called transport hysteresis. We found that the transport at a given location was not determined by the T_e gradient or T_e at that location. This hysteresis was confirmed repeated by turning the core heating on and off; the non-local nature of the non-diffusive heat transport associated with heat convection was experimentally revealed as T_e moved back and forth between peak, flat, and hollow profile states. This finding is a new insight into transport phenomena in fusion plasmas.

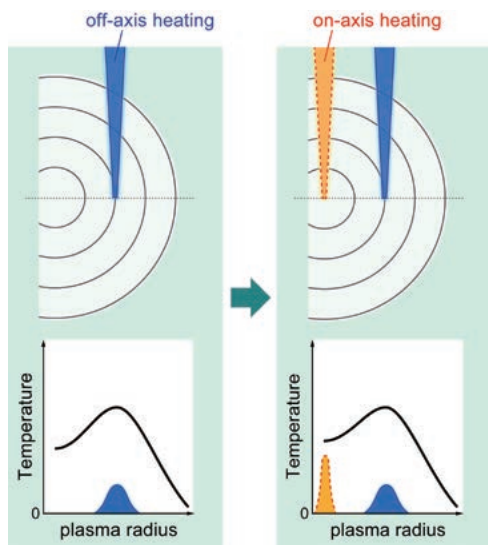


Fig. 1 Schematic diagram of a radial T_e profile during the modulated on-axis ECH, superimposed on the steady-state off-axis ECH.

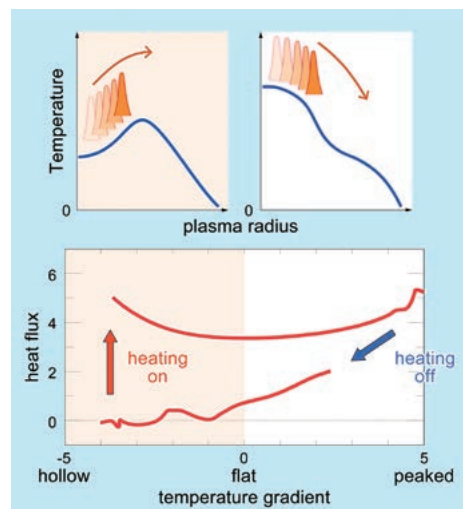


Fig. 2 Diagram of the flux-gradient relation when the non-locality of non-diffusive counter-gradient transport is present under the heat pulse, with the on-axis ECH propagating outward.

[1] T. I. Tsujimura *et al.*, Phys. Plasmas **29**, 032504 (2022).

(T. Tsujimura)

Impact of Magnetic Field Configuration on Heat Transport in Stellarators and Heliotrons

Optimization of magnetic configuration is one of the most important issues in stellarator/heliotron research. Neoclassical and anomalous transport, which are thought to be driven by turbulence, should be minimized in order to increase the confinement time. The optimization criteria can be obtained from comparison studies between LHD and W7-X, which currently represent the largest stellarator/heliotron. LHD is characterized by strong magnetic shear ($dt/d\rho$) and large effective helical ripple (ϵ_{eff}), while W7-X is characterized by weak $dt/d\rho$ and small ϵ_{eff} . These dissimilarities result in different characteristics of neoclassical and anomalous transports.

The plasma volume is almost 30 m^3 in both devices. Thus, comparison with the same heating power can clarify the difference of transport without any normalization. Figure 1 shows the comparison of density and temperature profiles of LHD and W7-X under identical experimental conditions. The magnetic configuration employed is an inward shifted configuration for LHD, where the magnetic axis position (R_{ax}) is 3.6 m at 2.75 T, and the standard configuration for W7-X is at 2.5 T. Heating is 2 MW electron cyclotron resonant heating (ECRH) and power deposition is localized in the central region in both devices. The averaged density is around $1.5 \times 10^{19}\text{ m}^{-3}$. Hollowed electron density (n_e) profiles in LHD and the peaked n_e profile in W7-X are one of the striking differences between the two. The central electron temperature (T_e) is higher in W7-X, while the T_e is higher in LHD at the outer mid-radius. The ion temperature (T_i) is higher in LHD in the entire region, while the T_i gradient is steeper in W7-X. Power balance analyses were carried out. The profiles of experimentally obtained ion thermal conductivities (χ_i^{EXP}) are shown in Fig. 2 (a) for W7-X and (b) for LHD, together with neoclassical ion thermal conductivities (χ_i^{NC}). As shown in Fig. 2 (a) and (b), χ_i^{EXP} are almost comparable in the outer mid radius, while χ_i^{NC} are clearly lower in W7-X. This is attributed to the neoclassical optimization of W7-X configuration. The anomalous contribution of ion thermal conductivity can be defined as $\chi_i^{\text{ANO}} = \chi_i^{\text{EXP}} - \chi_i^{\text{NC}}$. As shown in Fig. 2 (c), the resultant χ_i^{ANO} is much lower in LHD. This is in strong contrast to much lower χ_i^{NC} in W7-X. Theoretical validations using gyrokinetic simulations were performed using GKV for LHD and GENE for W7-X, including both kinetic ion and electron effects. Simulated ion thermal conductivities (χ_i^{Sim}) are shown in Fig. 2 (c). Excellent agreements were obtained both for LHD and W7-X, indicating that the anomalous process of ion transport is driven by ion temperature gradient turbulence. The gyrokinetic simulations suggest that the lower χ_i^{ANO} in LHD is due to stronger zonal flow generation. The obtained results indicate that turbulence reduction and neoclassical transport do not necessarily coincide. Further investigations are necessary to find which magnetic parameter or which combination of it is important, in order to reduce neoclassical and anomalous transport simultaneously.

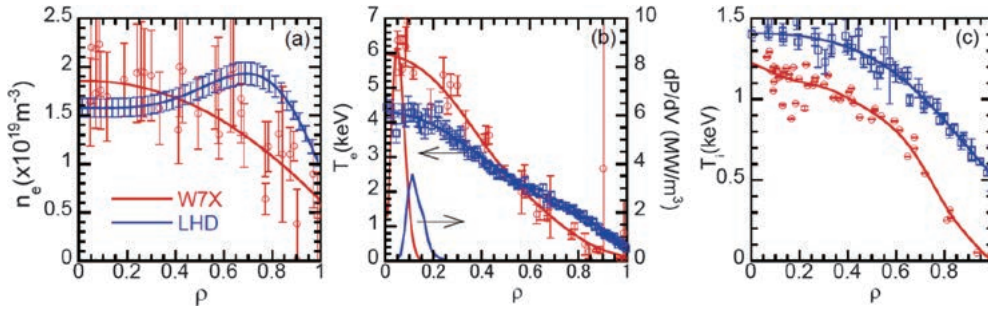


Fig. 1 Comparison of profile (a) n_e , (b) T_e and (c) T_i . ECRH power deposition profiles are shown in (b). LHD is the inward shifted configuration ($R_{\text{ax}}=3.6\text{ m}$) at 2.75 T, W7-X is the standard configuration at 2.5 T.

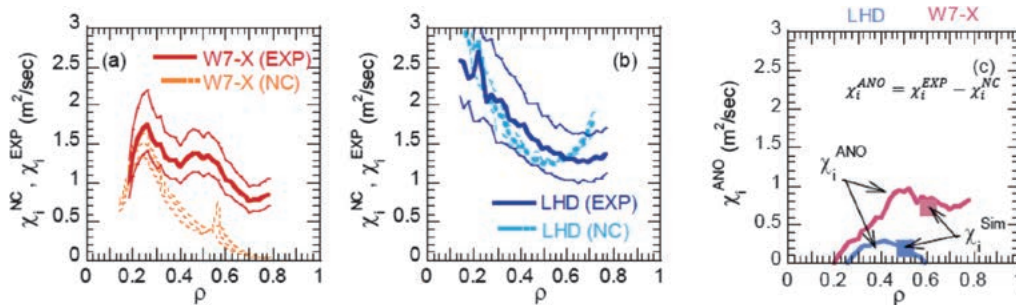


Fig. 2 Spatial profile of χ_i^{EXP} , χ_i^{NC} and χ_i^{ANO} . Plain and dashed line in (a) and (b) indicate χ_i^{EXP} and χ_i^{NC} respectively. In (a) and (b), upper and lower boundaries of estimation uncertainty are shown by thin lines. In (c), plain lines indicate χ_i^{ANO} , symbols indicate χ_i^{Sim} .

Plasma Spectroscopy

Highlight

Assessment of W density in LHD core plasmas using visible forbidden lines of highly charged W ions [1]

Tungsten (W) densities in core plasmas of the Large Helical Device (LHD) have been successfully assessed with measurements of optically forbidden magnetic-dipole (M1) lines in the near-ultraviolet region emitted by W^{26+} and W^{27+} in ground states (Fig. 1). The ground states of W^{26+} and W^{27+} have 4f valence electrons outside the palladium iso-electronic core (Fig. 2); the electron configurations are different from the ground state of any element in the periodic table. In a strong Coulomb field of tungsten nucleus, energy levels of the 4f valence orbitals are split by interaction with the electron spin. The observed emission lines in the near-ultraviolet region were due to M1 transitions between those levels. We constructed a collisional-radiative model for the M1 lines of highly charged tungsten ions in plasmas, to evaluate tungsten ion densities from the M1 line intensities. Based on the W^{26+} and W^{27+} densities, the spatial distribution of total tungsten density and its time evolution (Fig. 3) were assessed.

The present work showed the potential usefulness of visible forbidden lines for tungsten measurements in fusion plasmas.

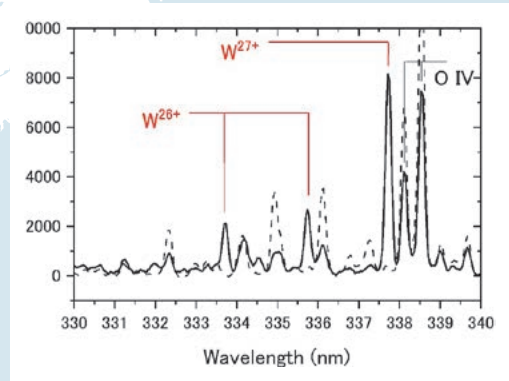


Fig. 1 Near-ultraviolet M1 lines of W^{26+} and W^{27+} (red bars) observed at the LHD. The solid line shows a spectrum observed with tungsten, and the dashed, a spectrum without tungsten.



Fig. 2 Ground state electronic configurations of neutral silver (Ag, $Z=47$), cadmium (Cd, $Z=48$), silver-like W^{27+} , and cadmium-like W^{26+} . W^{27+} and W^{26+} have 4f valence electrons and a palladium iso-electronic core: $[Pd]=1s^22s^22p^63s^23p^63d^{10}4s^24p^64d^{10}$.

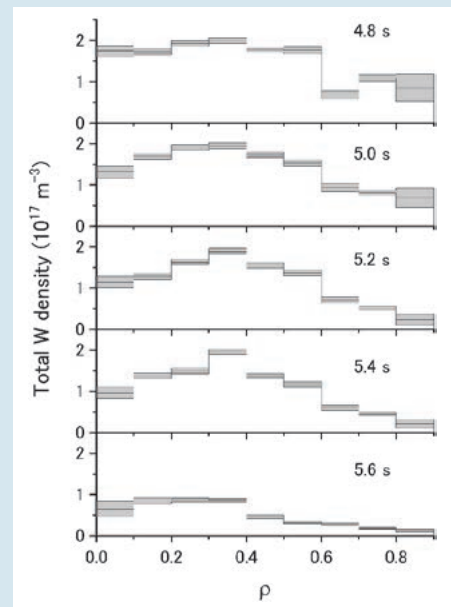


Fig. 3 Radial profiles of the total W density in the core at 4.8 – 5.6 s after W pellet injection at 4.0 s. ρ stands for a normalized minor radius measured from the center of a poloidal cross-section of the LHD. Gray zones represent uncertainty (1σ).

(D. Kato)

Simultaneous Observation of Tungsten Spectra of W^0 to W^{46+} Ions in Visible, VUV and EUV Wavelength Ranges in the Large Helical Device [2]

Spectroscopic studies for emissions released from tungsten ions have been conducted for a contribution to a tungsten transport study in tungsten divertor fusion devices and for expansion of the experimental database of tungsten line emissions (Fig. 4). Tungsten ions are distributed in the LHD plasma by injecting a pellet consisting of a small piece of tungsten metal wire enclosed by a carbon tube. Line emissions from W^0 , W^{5+} , W^{6+} , W^{24+} – W^{28+} , W^{37+} , W^{38+} , and W^{41+} – W^{46+} are observed simultaneously in visible (3200–3550 Å), vacuum ultraviolet (250–1050 Å), and extreme ultraviolet (5–300 Å) wavelength ranges, and the wavelengths are summarized. Temporal evolutions of line emissions from these charge states are compared for comprehensive understanding of tungsten impurity behavior in a single discharge.

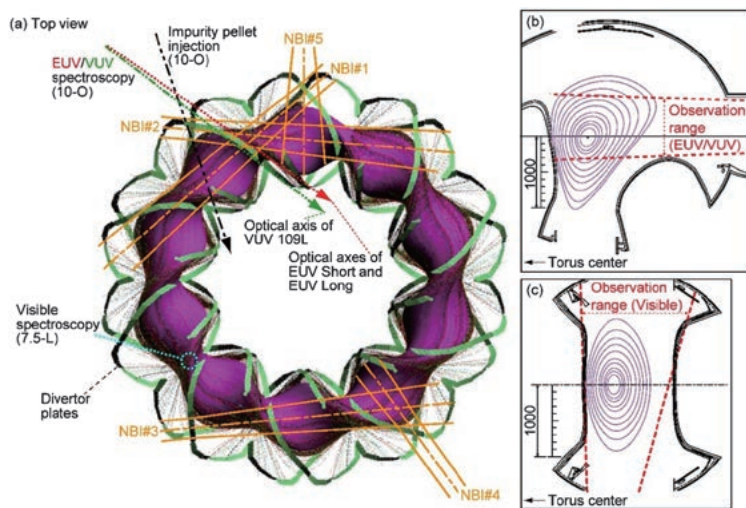


Fig. 4 (a) Top view of shape of plasma in LHD device together with schematic drawings of neutral beam injection (NBI) for heating, spectroscopic diagnostics, and impurity pellet injection. Cross-sections of magnetic surfaces where optical axes of (b) VUV/EUV and (c) visible spectroscopy systems are located, together with viewing angle of each system.

on the electron temperature (Fig. 5). Measurements of emissions from W^{10+} to W^{20+} are still insufficient, which is addressed as a future task.

(T. Oishi)

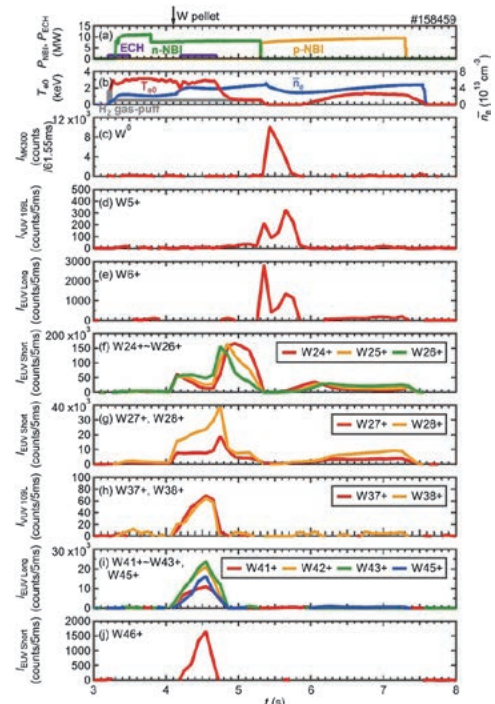


Fig. 5 Temporal evolution of (a) heating power of ECH, n-NBI, and p-NBI, (b) central electron temperature and line-averaged electron density, and W^0 – W^{46+} intensities integrated over wavelength ranges of (c) 3426.2–3427.9 Å for W^0 , (d) 637.8–641.2 Å for W^{5+} , (e) 261.0–261.5 Å for W^{6+} , (f) 32.15–32.30 Å for W^{24+} , 30.73–31.69 Å for W^{25+} , 29.29–30.40 Å for W^{26+} , (g) 28.58–28.69 Å for W^{27+} , 27.35–27.78 Å for W^{28+} , (h) 645.3–647.1 Å for W^{37+} , 558.6–560.3 Å for W^{38+} , (i) 131.0–131.3 Å for W^{41+} , 129.2–129.5 Å for W^{42+} , 126.1–126.5 Å for W^{43+} , 126.9–127.3 Å for W^{45+} , and (j) 7.89–7.95 Å for W^{46+} .

Spectra of Ga-like to Cu-like praseodymium and neodymium ions observed in the Large Helical Device [3]

Fifteen elements with atomic numbers of 57–71, called lanthanides, have a similar nature to each other. Regarding the emission spectra from highly charged lanthanide ions, available experimental data are still insufficient for some of the elements. The Large Helical Device (LHD) can be exploited for producing spectral data of highly charged heavy ions because high-temperature and high-emissivity plasmas can be stably generated, and impurity injection systems and advanced diagnostic systems are available.

In this study, we focus on extreme ultraviolet (EUV) emission spectra of highly charged praseodymium (Pr) and neodymium (Nd) ions, introduced into optically thin high-temperature plasmas produced in LHD. Discrete spectral lines emitted mainly from highly charged ions having 4s or 4p outermost electrons were observed in plasmas with electron temperatures of 0.8–1.8 keV (Fig. 6). Based on the recently published list of lines of neodymium ions in an electron beam ion trap (EBIT) experiment, most of the isolated lines of Ga-like to Cu-like praseodymium ions were identified as well from the similarity of the spectral features of the two elements. Some of them have been identified experimentally for the first time in LHD.

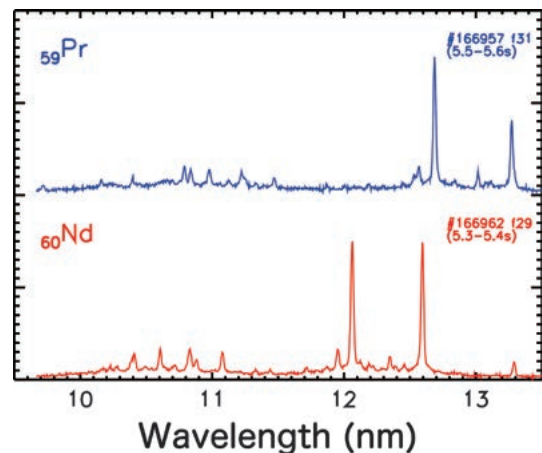


Fig. 6 Emission spectra of praseodymium (Pr) and neodymium (Nd) ions in the wavelength range of 10–13 nm, observed in high-temperature plasmas produced in the Large Helical Device (LHD). It is clearly seen that there are similar spectral structure shifts to shorter wavelengths in Nd (Atomic number: 60), in comparison with Pr (Atomic number: 59).

(C. Suzuki)

Z-dependent crossing of excited-state energy levels in highly charged galliumlike lanthanide atomic ions [4]

Extreme ultraviolet (EUV) optical transitions of lanthanide highly charged ions have been studied. The $[\text{Ni}]4s^24p - [\text{Ni}]4s^24d$ and $[\text{Ni}]4s^24p - [\text{Ni}]4s4p^2$ transition lines of galliumlike lanthanide elements have been spectroscopically measured in Large Helical Device (LHD) plasma and electron-beam ion trap (EBIT) plasma. Figure 7 gives the typical line spectra measured in LHD. The wavelengths for europium ions agree within 0.03% between the LHD and EBIT measurements. The precise spectroscopic data not only give useful knowledge for diagnostics of fusion plasma but also challenging subjects for atomic and molecular physics research. Due to the enhancement of spin-orbit interactions along with the increase of atomic number Z in $4p$ atomic orbitals, energy splitting between $4p_{-}$ (or $4p_{1/2}$) and $4p_{+}$ (or $4p_{3/2}$) orbitals increases significantly from lanthanum to lutetium, causing the crossing of Z -dependent wavelength curves. Figure 8 gives the Z -dependent level-crossing features. The relativistic effects are stronger in lower orbital angular momentum orbitals such as $4p$, because they stick to

the area of the atomic center; the effect of spin-orbit interaction is larger in the electron configurations with lower orbital angular momentum orbitals. The spectral line positions and strengths are theoretically calculated by means of the multi-configuration Dirac-Fock method. The mixing of the $[\text{Ni}]4s^24d_-$ and $[\text{Ni}]4s4p_+^2$ configurations leads to an avoided crossing in the apparent wavelength curves. The configuration mixing makes both the $[\text{Ni}]4s^24p_- - [\text{Ni}]4s^24d_-$ and originally optically forbidden $[\text{Ni}]4s^24p_- - [\text{Ni}]4s4p_+^2$ lines well visible in the EUV spectra near the level crossing point. The levels are found to cross between $Z = 62$ and 63 .

(F. Koike)

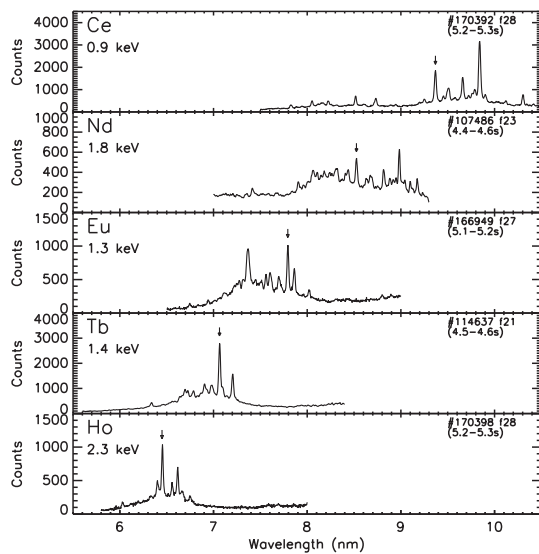


Fig. 7 Discrete EUV emission spectra of highly charged Ce, Nd, Eu, Tb, and Ho ions in LHD. The vertical arrows indicate the lines due to the transition $[[\text{Ni}]4s^24p_-]_{1/2} - [[\text{Ni}]4s^24d_-]_{3/2}$ of Ga-like ions. The central electron temperature associated with each spectrum is shown in each panel.

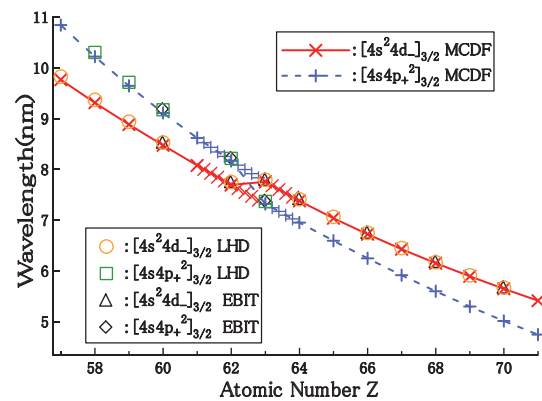


Fig. 8 Wavelength for the transitions of Ga-like ions of lanthanide elements with $Z = 57-71$ (La to Lu). Solid (red) line and symbol \times , present MCDF calculation; open (orange) circle, LHD experiment; open (black) triangle, EBIT experiment for the $[[\text{Ni}]4s^24p_-]_{1/2} - [[\text{Ni}]4s^24d_-]_{3/2}$ transition. Broken (blue) line and symbol $+$, present MCDF calculation; open (green) square, LHD experiment; open (black) diamond, EBIT experiment for the $[[\text{Ni}]4s^24p_-]_{1/2} - [[\text{Ni}]4s4p_+^2]_{3/2}$ transition.

- [1] D. Kato *et al.*, Nuclear Fusion **61**, 116008 (2021).
- [2] T. Oishi *et al.*, Atoms **9**, 69 (2021).
- [3] C. Suzuki *et al.*, Atoms **9**, 46 (2021).
- [4] F. Koike *et al.*, Phys. Rev. A **105**, 032802 (2022).

Annual Report of Instability TG

Highlight

Observation of self-sustained divertor oscillation driven by magnetic island dynamics in LHD

In magnetically confined plasmas, a magnetic island, an isolated magnetic field structure embedded in nested tori, occasionally forms. In the Large Helical Device (LHD), the magnetic island can be externally induced by perturbation coils installed outside the device, in order to study interaction between plasma and the magnetic island. One of the outcomes in forming the magnetic island is that plasma radiation is distinguishably enhanced at a specific point of the magnetic island (the so-called X-point) and the plasma heat load onto the plasma-facing materials is significantly mitigated, maintaining core plasma performance. This operation regime, the so-called detached state, is beneficial for fusion reactor development. The background physics of this operation regime is studied in detail.

In LHD, oscillations in the magnetic island width at a constant frequency (several tens of Hertz) were discovered. This oscillation was driven by a continuous power input, and was called self-sustained oscillation. The oscillations were also found in the divertor heat load and radiation losses therefore, were considered to be sequential detachment transitions and back-transitions. In order to analyze the background physics, a model used in biology, the so-called predator-prey model, was used. The model was composed by nonlinearly coupling two equations: one for the magnetic island dynamics (modified Rutherford equation) and the other for the bootstrap current (an empirical model). According to the model, the following interpretation was made possible. Once the magnetic island extends, the X-point radiation is enhanced and eventually a detachment transition occurs. In the detached phase, high X-point collisionality impedes the X-point remnant bootstrap current, and then the magnetic island starts to shrink. The plasma returns to the attached phase and the X-point collinearity decays. As a result, the X-point remnant bootstrap current recovers and the magnetic island again starts to grow. Schematic of this interpretation is overviewed in Figure 1. By numerically examining the system equation, it was found that the model can qualitatively explain the observation [1].

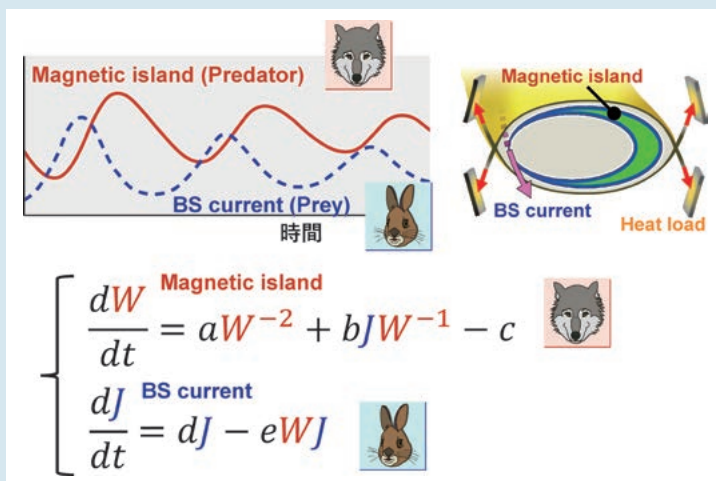


Fig. 1 Schematic of predator-prey model in divertor oscillation: (Left top) competition between magnetic island and bootstrap (BS) current, (Right top) illustration of geometry, and (Bottom) equations describing two variables ($a-e$ are constants).

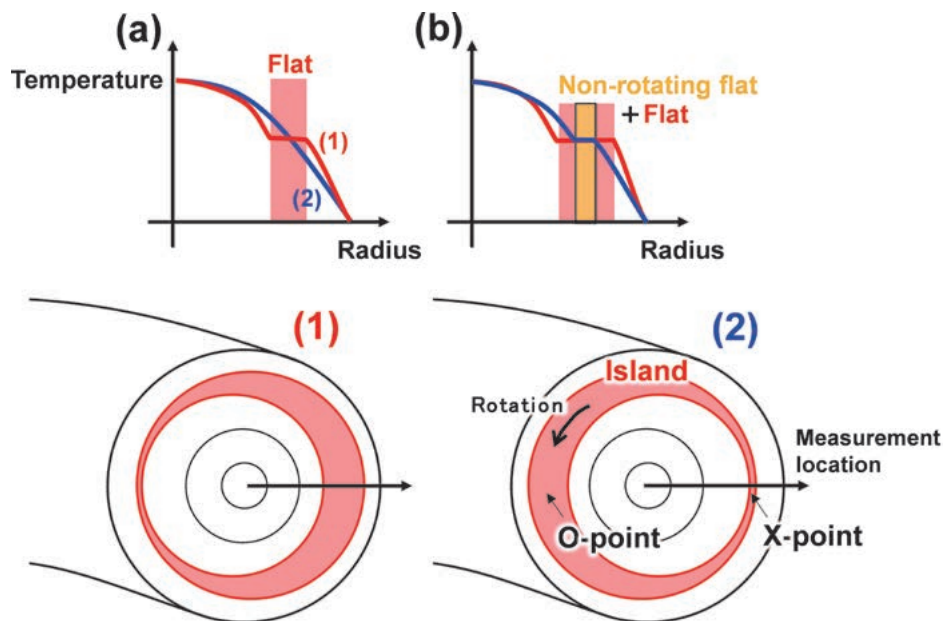
[1] T. Kobayashi *et al.*, Phys. Rev. Lett. **128**, 085001 (2022).

First observation of characteristic fine structure of MHD fluctuations with decreasing frequency

In magnetic confinement plasmas, rapid growth of MHD fluctuations after a decrease in frequency of these fluctuations is one of key problems. In order to clarify the frequency decreasing mechanism in the LHD, fine local electron temperature profiles were measured by using the Thomson scattering system with a high-repetition-rate Nd:YAG laser.

Figure (a) shows the schematic view of electron temperature profiles in the first stage of the slowing-down phase, a flattening (red line) or tilting (blue line) structure in temperature profiles was repeatedly observed with the time. If a magnetic island is formed, in the region called the O point of the magnetic island, the temperature profile is flattened, but at the X point, the effect on the temperature profile is small. Therefore, the above result suggests that the magnetic island rotates with plasma.

On the other hand, in the last stage of the slowing-down phase as shown in Figure (b), it was found for the first time that some of the region constantly flattens (yellow hatched area). This result suggests a possibility that there is a non-rotating magnetic field formed the non-rotating island, and the interaction between it and a perturbed current due to instability leads to the $\mathbf{j} \times \mathbf{B}$ braking torque [1].



[1] Y. Takemura *et al.*, Plasma Fusion Res. **16**, 1402091 (2021).

(Y. Takemura)

Analysis of NB Fast-Ion Loss Mechanisms in MHD Quiescent LHD Plasmas

The beam-ion loss mechanism in the Large Helical Device (LHD) has been analyzed quantitatively by using neutron measurement and integrated simulation. It had been expected that “neo-classical transport” was dominant as the beam ion loss mechanism in LHD, the same as in large size tokamaks. In this paper, it was clarified that neo-classical simulation not can reproduce the experimental results in LHD, contrary to tokamak cases. In figure 1, the x axis indicates the neutron decay time, assuming no fast-ion loss and the y axis indicates the measured (blank) and simulated (filled) neutron decay time. The decay of neutrons generated by a DD fusion reaction comes from the two components. One is fast-ion slowing down, the other is the fast-ion loss. In fig. 1, these two components are separated by simulation. If fast ions are confined perfectly, data should be distributed along the $y = x$ line. and data should be distributed along the line. If fast ions are lost with the time constant, data should be distributed on the fitting curve. As shown in fig. 1, the neo-classical simulation results are distributed along a line contrary to the experimental results. This result indicates that the other mechanism is as dominant as the beam ion loss mechanism in LHD. According to our preliminary analysis, the most plausible candidate for the dominant fast-ion loss mechanism is charge exchange (CX) loss. An accurate quantitative estimation of the CX loss is difficult because neutral particle density, which is crucial for the estimation of CX reactivity in the plasma core region, not can be measured. Detailed discussion about the CX loss estimation is to be found in future work.

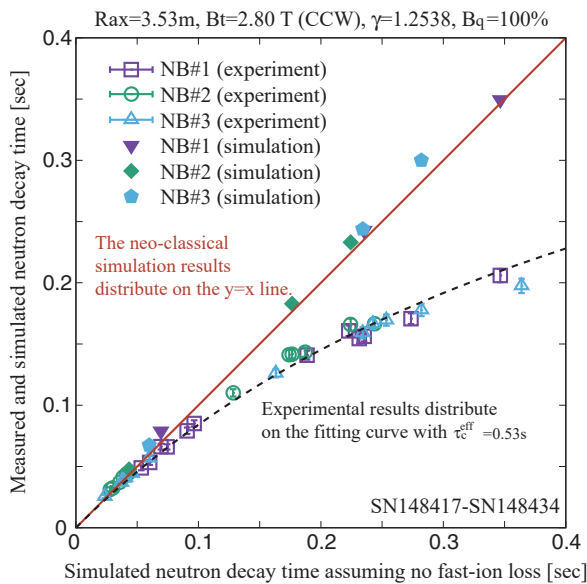


Fig. 1 Comparison between the experimental results and the neo-classical simulation results.

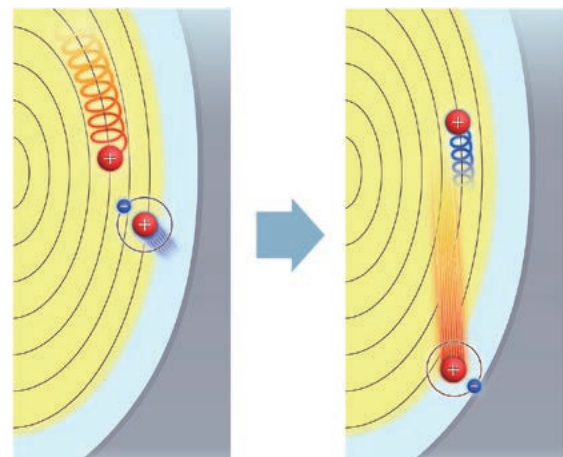


Fig. 2 A conceptual image of the CX loss. A fast-ion loses its charge due to CX loss and then the neutralized fast-ion is lost from the magnetic field.

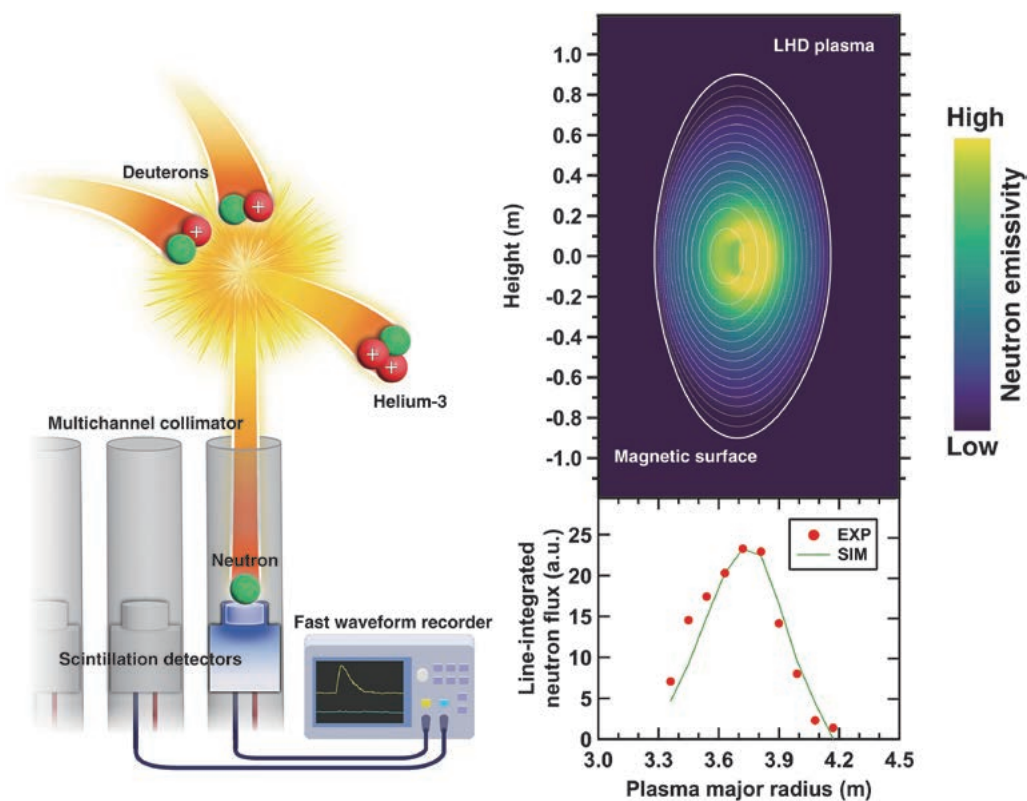
(H. Nuga)

Measuring the spatial distribution of energetic particles in a deuterium plasma

In this study, we focused on how the neutral beam injection (NBI) direction and the magnetic field strength affect the spatial distribution of energetic particles by utilizing neutron emission profile diagnostics, recorded by a vertical neutron camera [1].

The vertical neutron camera was utilized to measure neutron emission profiles in LHD deuterium plasmas with tangential NBI under various magnetic field conditions. The peak of the line-integrated neutron profile shifts outward in the co-injection case and inward in the counter-injection case. The shift becomes more significant when the magnetic field decreases in strength.

We compared the observed neutron emission profile in the experiment and it was calculated by a guiding center orbit following simulation DELTA5D [2]. The shapes of the neutron emission profile, calculated for high and medium field strength conditions, were in good agreement with those obtained experimentally, and the numerical simulations were validated for LHD [3].



[1] K. Ogawa *et al.*, Rev. Sci. Instrum. **89**, 113509 (2018).

[2] D. A. Spong, Phys. of Plasmas **18**, 056109 (2011).

[3] K. Ogawa *et al.*, Plasma Phys. Control. Fusion **63**, 065010 (2021).

Research and Development Collaboration Program for LHD-Project

An RF induced transport model for the study of RF wave sustained plasmas

An RF transport model is constructed to understand the energy, momentum and particle confinement properties of lower hybrid wave sustained plasmas. Using the model, major properties of RF wave sustained TST-2 spherical tokamak plasmas are reproduced. The reproduction indicates that electrons are accelerated by the RF wave, and simultaneously transported toward a limiter and are lost.

Plasma current generation and sustainment by an RF wave are important issues for spherical tokamak research. In most of the experiments so far, the obtained plasma density and the plasma current are relatively low. In such a case, RF induced transport of high energy electrons can be the dominant process determining the energy, momentum (i.e., current) and particle confinement of electrons. In the constructed model, the velocity evolution of an electron is obtained through the equation $\Delta V_{\parallel} = \Delta \tilde{V}_{\parallel} - v_{\parallel} V_{\parallel} \Delta t - \frac{eE}{m} \Delta t$, where the terms in the RHS represent a random velocity change due to the RF wave, collisional slowing down and acceleration by electric field, respectively. The orbit of an electron can be calculated from the velocity, and the electron is lost when the orbit touches one of the limiters. The electron velocity distribution function (EVDF) is obtained by following many electrons, and the plasma current, the deposited RF power, energy and particle confinement times are calculated from the EVDF. Some model parameters are adjusted to reproduce the measured plasma current, electron density and RF wave power. The model results suggest that a major fraction of the deposited RF power, which generates fast electrons, is lost by the electrons hitting a limiter, while a minor fraction is used to heat bulk electrons and ions. From the energy distribution of the lost electrons, we can calculate the hard X-ray generation and the energy spectrum of measured hard X-rays. Figure 1 shows the calculated and the experimental hard X-ray spectra, and qualitative agreements between the experimental and the model results are shown.

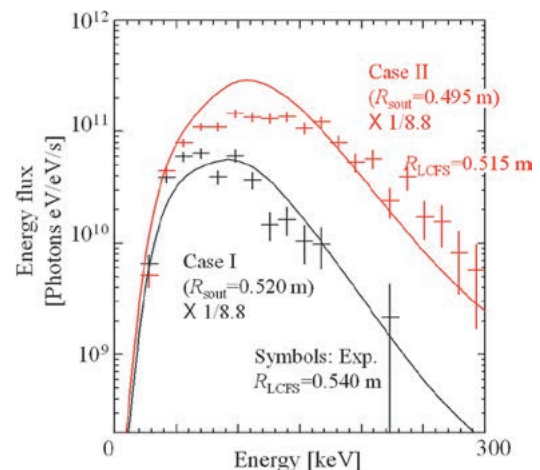


Fig. 1 Calculated (solid curve) and experimental (plus symbols) energy spectra. The calculated spectra are obtained by using the energy distribution of lost electrons in the model. They are multiplied by a factor of 1/8.8 in the plot to reproduce the experimental spectra. Two cases with different plasma sizes are shown by black and red. [1]

[1] A. Ejiri *et al.*, “A Fast Electron Transport Model for Lower Hybrid Wave Sustained Plasmas”, *Plasma and Fusion Research* **17**, 1402037 (2022).

(A. Ejiri)

Spatially resolved measurements of SOL electron temperature and density using near-infrared Zeeman spectroscopy

In fusion-related toroidal plasmas, emission spectroscopy is used for plasma control and machine protection by measuring impurity generation and transport, confinement mode transition, the hydrogen isotope ratio, neutral density, and so forth. These diagnostics have however, a drawback that they can measure only the viewing-chord-integrated spectrum. To obtain a spatially resolved spectrum, additional methods such as computer-aided

tomography, with more than two directional observations, using multiple viewing chords or active emission spectroscopy, for detecting a neutral beam or laser-induced emission from the intersection between the beam and the viewing chord are required. The application of these methods will however, become difficult in future fusion reactors owing to a limitation in the available port area. It is thus desirable to develop an alternative method that is implementable by using a single diagnostic port.

A method that can satisfy this requirement is Stokes spectropolarimetry, which is widely used in the fields of astrophysics and ellipsometry. It determines the polarization state of an emission line spectrum by measuring the Stokes parameters I , Q , U , and V of this spectrum. Particularly for plasma spectroscopy, Stokes spectropolarimetry can be used as a method to spatially invert the viewing-chord-integrated spectrum, on the basis of the correspondence between the given magnetic field profile along the viewing chord, and the Zeeman effect appearing on the spectrum. Its application to fusion-related toroidal plasmas is however, limited, owing to low spatial resolution as a result of the difficulty in distinguishing between the Zeeman and Doppler effects. To resolve this issue, we increased the relative magnitude of the Zeeman effect by observing a near-infrared emission line on the basis of the greater wavelength dependence of the Zeeman effect than of the Doppler one.

The measurement was applied to the HeI 2^3S - 2^3P emission line from a helium-puffed deuterium plasma produced in Heliotron J (Fig. 1(a)). Owing to the enhancement of the Zeeman effect relative to the Doppler one, the former was conspicuously observed at a magnetic field strength smaller than those used in other devices. By utilizing the Zeeman effect, we were able to reproduce the chord-integrated spectrum by a simulation with empirically optimizing recycling conditions of atoms at the first walls (Fig. 1(b)). In a future study, we intend to spatially resolve multiple near-infrared HeI emission line spectra and evaluate the spatially resolved SOL electron temperature and density using collisional-radiative model analysis.

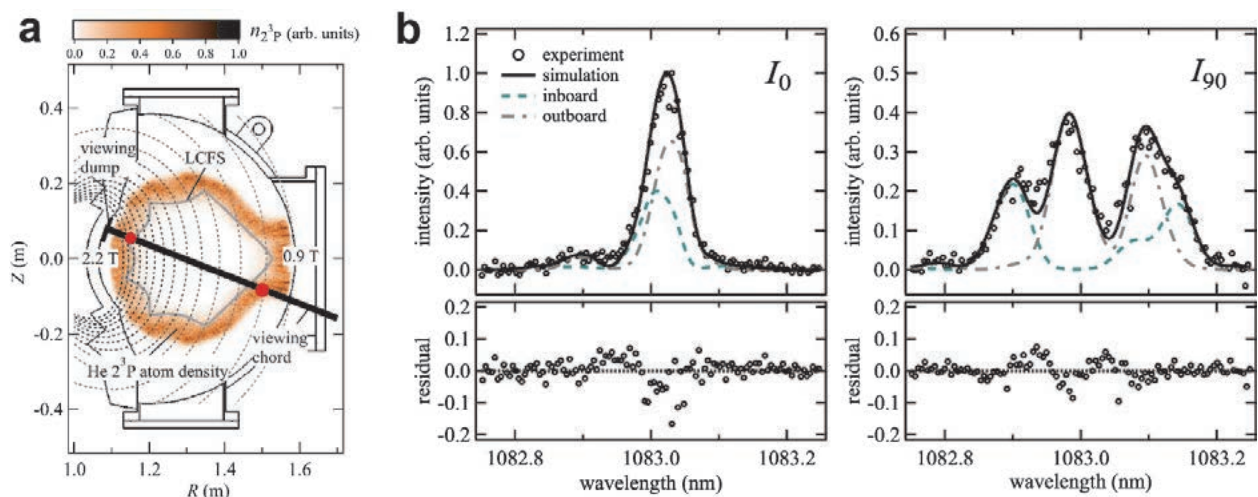


Fig. 1 (a) #10.5 poloidal plane of Heliotron J with a viewing chord. The magnetic field strength of 0.9–2.2 T is shown by dashed lines. The relative 2^3P excited helium atom density obtained by simulation is shown by the color map and the emission locations and relative intensities determined using the two-point emission model adopted in early studies of spatial inversion are plotted with red circles. (b) Orthogonal linear polarization spectra, I_0 and I_{90} , which are nearly parallel and perpendicular to the magnetic field, respectively, of a chord-integrated HeI 2^3S - 2^3P emission line spectrum averaged over 10 discharges (#80303–312). The lines show the fitted spectra obtained by a simulation with optimizing recycling conditions of atoms at the first walls. Figures are cited from T. Chatani, T. Shikama *et al.*, *Sci. Rep.* **12**, 15567 (2022); doi:10.1038/s41598-022-19747-8.

(T. Shikama)